X-ray scattering by rare-earth multipoles in multiaxial structures

1998 J. Phys.: Condens. Matter 10 9875

(http://iopscience.iop.org/0953-8984/10/43/032)

J. Phys.: Condens. Matter **10** (1998) 9875–9888. Printed in the UK PII: S0953-8984(98)95156-6

X-ray scattering by rare-earth multipoles in multiaxial structures

M Amara and P Morin

Laboratoire Louis Néel†, CNRS, BP 166X, 38042 Grenoble Cédex, France

Received 17 June 1998

Abstract. The Thompson scattering of x-rays is a direct probe for the electronic charge distribution of atoms. It should then be useful for determining types of ordering which involve a periodical asphericity of the atoms inside a crystal. We focus on the case of the periodical multiaxial orientation of the 4f shells in a rare-earth compound. Using the Stevens equivalent-operator method, the formalism of the multipolar scattering is here developed within the ground-state multiplet of the rare-earth ion. It allows one to consider proper 4f wave functions, accounting for the various interactions present in the system, and to calculate the quadrupolar, octupolar and dodecapolar contributions to the scattering. In order to validate this x-ray technique, we propose its application to compounds presenting magnetic orderings which coincide with multiaxial orbital arrangements.

1. Introduction

In relation with the development of high flux x-ray sources, diffraction experiments giving details of the electronic charge distribution may be envisaged. For instance, it brings the opportunity of measuring weak Bragg reflections due to a periodical aspherical charge density. In this regard, first diffraction experiments were carried out on holmium, as early as the late sixties, by Keating [1]. However, this work found little continuity, presumably in relation with the intrinsically weak signal and the difficulties of the analysis.

In the disordered phase of rare-earth compounds, the 4f electronic distribution reflects the point symmetries of the lattice. The pair interactions between the 4f shells drive orderings in which their electronic density no longer respects the initial symmetries: the dominant modification of the asphericity is described by additional quadrupolar components. If the lattice translational symmetries are preserved, the arrangement is called ferroquadrupolar. This ($\boldsymbol{q} = \mathbf{0}$) order is accompanied by a macroscopic lattice distortion, according to the strength of the magnetoelastic couplings. Such an arrangement is generally the consequence of a collinear magnetic ordering, but it can also result from a cooperative Jahn–Teller effect, or may spontaneously develop due to strong quadrupolar pair-interactions [2]. This is, for instance, the case of the CsCl-type compound TmCd, which displays a phase of pure ferroquadrupolar order, the rare-earth magnetic moment remaining zero at all sites [3].

Another type of ordering, in some way reminiscent of the antiferromagnetic order, consists of an arrangement of the quadrupoles with a periodicity which differs from the

† Associated with the Joseph Fourier University of Grenoble.

0953-8984/98/439875+14$19.50

crystallographic one. Such an arrangement, called antiferroquadrupolar, also derives from a magnetic order or from strong antiferroquadrupolar couplings.

Actually, an antiferroquadrupolar arrangement, described by only ($\boldsymbol{q} \neq \mathbf{0}$) wave vectors, has no direct macroscopic signature. As for the antiferromagnetic order, the ideal probe should be microscopic, but neutron diffraction is of little interest as one considers the scattering by an electronic charge distribution. However, attempting to overcome this limitation of the neutron diffraction, different techniques have been developed.

An analogue of the Keating experiment has been carried out using neutron scattering, probing the asphericity of the magnetization density through the periodical form factor [4]. The disadvantage of this technique lies in the non-trivial relation between charge and magnetic densities.

Magnetic neutron diffraction has been used in order to characterize the antiferroquadrupolar phase of the cubic CeB_6 compound, taking advantage of the ferrimagnetic structure induced by applying a magnetic field [5]. Indeed, this magnetic field induces different paramagnetic moments on the Ce sites which are no longer equivalent in the antiferroquadrupolar phase. However, this is again an indirect technique which requires an external stress and does not unambiguously reveal the quadrupolar structure. This latter has to be deduced from the ferrimagnetic structure, which does not insure a unique determination. Up to now, the real nature of the quadrupolar order of CeB_6 remains an open question (see [6]). In particular, to which of the cubic representations, Γ_3 or Γ_5, the ordered quadrupolar components belong is not yet answered.

In the hexagonal UPd_3 compound, Walker *et al* [7] have analysed the outbreak of tiny neutron diffraction peaks as resulting from periodical displacements of the atoms in relation with a quadrupolar ordering. However, as soon as the quadrupolar structure preserves the ordered sites as symmetry inversion centres, such a periodical displacement mode cannot result from the quadrupolar order alone. It requires a pre-existing lattice instability, which manifests itself in coincidence with the quadrupolar ordering, as an additional symmetry breaking. Therefore, such a method cannot be regarded as a general probe for antiferroquadrupolar orderings.

Other antiferroquadrupolar structures have been assumed to exist in rare-earth compounds as $PrPb_3$, $TmGa_3$ [8] or TmTe [9]. In these compounds, however, the actual quadrupolar structures are not unambiguously known. Although it is an intrinsically weak phenomenon, the x-ray diffraction by electric quadrupoles appears as the most direct technique for solving many of these questions.

In order to validate this technique, we propose to verify it experimentally in normal rare-earth systems, for which the multiaxial magnetic structures, thus the quadrupolar ones, are well characterized. Indeed, the direct use of x-ray diffraction on the above mentioned rare-earth systems appears rather delicate, both from technical and fundamental points of view. $PrPb_3$ orders below 0.3 K and the presumed antiferroquadrupolar range of $TmGa_3$ is only 0.04 K wide, immediately above T_N. In the case of CeB_6, the Kondo coupling complicates the analysis and the same is valid for TmTe, where a change of valence occurs. The advantage of using a multiaxial magnetic structure is that the coexisting quadrupolar arrangement can be deduced, once the magnetic structure has been unambiguously determined from neutron diffraction measurements (section 2). One has then an archetype of antiferroquadrupolar structure, for which the location of the quadrupolar diffraction peaks is perfectly determined and their intensities predictable within a microscopic model (section 3). Reciprocally, the technique would also be valuable for demonstrating the multiaxial character of spontaneous magnetic structures, without need of an external stress.

2. Magnetic and quadrupolar structures

The essential point is here to establish the connection between a given multiaxial antiferromagnetic structure and the coexisting quadrupolar structure. Even in the hypothetical absence of quadrupolar couplings, a magnetic ordering would be accompanied by the development of quadrupolar components on the magnetic sites (except, obviously, for systems with zero total orbital moment). This is a direct consequence of the local magnetic symmetry-lowering. There is then a single quadrupolar arrangement compatible with the observed magnetic structure (this is not, however, a one-to-one relation, since the same quadrupolar arrangement may correspond to several magnetic structures). In the case of isotropic magnetic exchange, this particular structure stabilizes because the associated quadrupolar arrangement is the most favourable one with regard to the quadrupolar couplings [10].

Before developing the relation between the magnetic structure and the quadrupolar arrangement, it may be useful to recall the fundamentals regarding the multiaxial magnetic structures and the description of the quadrupolar moments in rare-earth systems.

2.1. Magnetic high-symmetry structures

We consider the case of structures developing spontaneously on a simple cubic lattice of magnetic ions and restrict ourselves to the ones for which the magnetic sites remain equivalent in the ordered phase. To fulfil the conditions imposed by the crystalline-electric-field anisotropy, the magnetic moments are along directions within an exclusive $\langle 1\,0\,0\rangle$, $\langle 1\,1\,0\rangle$ or $\langle 1\,1\,1\rangle$ cubic star. The eigenstates describing the ions at two distinct sites can then be deduced one from another using a cubic point-group symmetry. One of the consequences is that the amplitude of the magnetic moment is the same on all sites. Such structures represent, at least at low temperatures, the majority of the antiferromagnetic orderings observed in simple-cubic systems.

In order to detail the relation between the magnetic and quadrupolar structures, we further reduce the scope of the discussion to magnetic structures with a period equal to or twice the cubic lattice along each of its three edges. Such magnetic structures are described using wave vectors from the $\langle 1/2\ 0\ 0\rangle$, $\langle 1/2\ 1/2\ 0\rangle$ and $\langle 1/2\ 1/2\ 1/2\rangle$ stars. Minimizing the bilinear energy requires the structure to involve a unique star of wave vectors, in correspondence with the maximum of the bilinear coupling dispersion curve. One should then consider the spontaneous structures exclusively based on the $\langle 1/2\ 0\ 0\rangle$ or $\langle 1/2\ 1/2\ 0\rangle$ stars. Note that the $\langle 1/2\ 1/2\ 1/2\rangle$ star reduces to a single branch and is not compatible with a multiaxial ordering. These so-called high-symmetry structures have been exhaustively listed in [10] and the literature provides numerous examples of their existence. Their Fourier description needs a maximum of three real components, perpendicular to each other in order to keep the moment amplitude constant from site to site. The magnetic moment at site j, located by $\boldsymbol{R}_j$, is expressed as

$$\langle \mathcal{M}\rangle_j = \boldsymbol{M}_1\,\mathrm{e}^{\mathrm{i}\boldsymbol{k}_1\cdot\boldsymbol{R}_j} + \boldsymbol{M}_2\,\mathrm{e}^{\mathrm{i}\boldsymbol{k}_2\cdot\boldsymbol{R}_j} + \boldsymbol{M}_3\,\mathrm{e}^{\mathrm{i}\boldsymbol{k}_3\cdot\boldsymbol{R}_j} \tag{1}$$

where $\boldsymbol{k}_1$, $\boldsymbol{k}_2$ and $\boldsymbol{k}_3$ are the three independent branches of the wave vector star and $\boldsymbol{M}_1$, $\boldsymbol{M}_2$ and $\boldsymbol{M}_3$ the respective Fourier components.

2.2. Quadrupolar operators

Excluding the existence of an electric dipole, the quadrupolar moments are the lowest-order description of a charge distribution's asphericity. The first and second columns of table 1

Table 1. The quadrupolar operators and their Stevens' equivalents (after [11] and [12]). The summations are over the 4f electrons, α_J is the Stevens multiplying factor and $\langle r^2 \rangle$ the 4f second-order radial integral.

Cartesian coordinates	Polar coordinates	Equivalent $\|J, J_z\rangle$ operator
$Q_2^0 = \sum_j 3z_j^2 - r_j^2$	$Q_2^0 = \sum_j r_j^2(3\cos^2\theta_j - 1)$	$\alpha_J\langle r^2\rangle[3J_z^2 - J(J+1)] = \alpha_J\langle r^2\rangle O_2^0$
$Q_2^2 = \sum_j x_j^2 - y_j^2$	$Q_2^2 = \sum_j r_j^2 \sin^2\theta_j(\cos^2\varphi_j - \sin^2\varphi_j)$	$\alpha_J\langle r^2\rangle[J_z^2 - J_y^2] = \alpha_J\langle r^2\rangle O_2^2$
$Q_{xy} = \sum_j x_j y_j$	$Q_{xy} = \sum_j r_j^2 \sin^2\theta_j \cos\varphi_j \sin\varphi_j$	$\alpha_J\langle r^2\rangle \left[\dfrac{J_xJ_y + J_yJ_x}{2}\right] = \alpha_J\langle r^2\rangle P_{xy}$
$Q_{yz} = \sum_j y_j z_j$	$Q_{yz} = \sum_j r_j^2 \sin\theta_j \sin\varphi_j \cos\theta_j$	$\alpha_J\langle r^2\rangle \left[\dfrac{J_yJ_z + J_zJ_y}{2}\right] = \alpha_J\langle r^2\rangle P_{yz}$
$Q_{zx} = \sum_j x_j z_j$	$Q_{zx} = \sum_j r_j^2 \sin\theta_j \cos\varphi_j \cos\theta_j$	$\alpha_J\langle r^2\rangle \left[\dfrac{J_zJ_x + J_xJ_z}{2}\right] = \alpha_J\langle r^2\rangle P_{zx}$

give the classical expressions of the five quadrupolar moments in terms of Cartesian and polar coordinates.

In a quantum description of the atom, the quadrupolar components become operators acting, through the electron coordinates, on the N-electron wave function. Using an N-electron determinantal wave function implies extremely tedious calculation [1] and is not common in 4f magnetism. Indeed, the atomic configuration of lowest energy is usually well described according to Hund rules. Thus the atomic state may be described using the multiplet representation associated with the total electronic angular momentum J. The quadrupolar operators are then expressed using momentum operators, according to the Stevens equivalent-operator method [11]. The correspondence between the N-electron and the $|J, J_z\rangle$ quadrupolar operators is detailed in table 1. It is worth noting that the operator equivalence is actually based on the correspondence between angular operators, acting on the N-electron wave functions, and momentum operators, acting on $|J, J_z\rangle$ states. The Stevens multiplying factor α_J insures the equality between a quadrupolar matrix element over a $|J, J_z\rangle$ state and its counterpart over the electron angular wave functions. The radial part of the quadrupolar operators, which is separated from the angular part in the polar expressions of table 1, acts identically on all the electron radial wave functions. Thus, it reduces to the $\langle r^2\rangle$ factor, which represents the integral of r^2 over the 4f electron radial wave function and is unaffected by the asphericity.

As only 4f shells are considered here, i.e. for an electronic orbital momentum $l = 3$, the full description of the atomic asphericity is achieved using distribution operators up to the sixth order. Starting from a real combination of spherical harmonics, fourth ($n = 4$) and sixth ($n = 6$) order multipolar operators may be defined, as well as their $O_n^{m(c,s)}$ Stevens equivalent operators [12]:

$$\begin{aligned} O_n^0 &\equiv C_n \sum_j Y_n^0(\theta_j, \varphi_j) \\ O_n^{mc} &\equiv C_n \frac{1}{\sqrt{2}} \sum_j [Y_n^{-m}(\theta_j, \varphi_j) + (-1)^m Y_n^m(\theta_j, \varphi_j)] \\ O_n^{ms} &\equiv C_n \frac{\mathrm{i}}{\sqrt{2}} \sum_j [Y_n^{-m}(\theta_j, \varphi_j) - (-1)^m Y_n^m(\theta_j, \varphi_j)] \end{aligned} \tag{2}$$

where the summations are over the 4f electrons, $m > 0$, $C_4 = \frac{16}{3}\sqrt{\pi}$ and $C_6 = (32/\sqrt{13})\sqrt{\pi}$. The $|J, J_z\rangle$ expressions for the $O_n^{m(c,s)}$ operators may be written using the spherical harmonics equivalent operators which have been listed by Buckmaster in [13].

2.3. From the magnetic to the quadrupolar structure

In case of a rare-earth ion located at a site of cubic symmetry, all the expectation values of the quadrupolar operators cancel. However, as soon as the system orders magnetically, the local symmetry is no longer cubic. One can consider the 4f shell as being under the influence of both a cubic environment and a mean magnetic field. For the high-symmetry magnetic structures, this field will either act along a fourfold, a twofold or a threefold axis (section 2.1). The new magnetic point group contains all elements of the cubic point group which preserves this field, including the elements which associate time reversal with a cubic space transformation. In addition to the magnetic moment, some quadrupolar components should develop in agreement with the new local symmetry. The quadrupolar operators, acting only through the electron coordinates, are insensitive with regard to time reversal. Thus, to determine the ordered quadrupolar components, one has only to consider the cube's symmetry subgroup preserving the local field axis, i.e. the magnetic moment axis.

In the case of a magnetic structure with moments along fourfold axes, the local cube's symmetry subgroup to be considered is D_{4h}. At a given j site located by $\boldsymbol{R}_j$, let us choose a local $(\hat{\boldsymbol{x}}_j, \hat{\boldsymbol{y}}_j, \hat{\boldsymbol{z}}_j)$ trihedron with, as z-axis, the magnetic moment direction, the x- and y-axes being taken along the two other edges of the cube. One observes that the five-dimensional quadrupolar representation is reducible into three one-dimensional, $\{(3z^2-r^2), (xy), (x^2-y^2)\}$, and one two-dimensional, (yz, zx), irreducible representations. However, among the one-dimensional representations, only one is fully symmetric and corresponds to $(3z^2-r^2)$. Thus, in terms of Stevens equivalent operators, the only quadrupolar component preserved in all symmetry operations is $\langle O_2^0 \rangle$. This component is then the only one having non-zero value as result of the magnetic order. Obviously, in agreement with the already mentioned assumptions, this quadrupole will have the same statistical value $Q_0 = \langle O_2^0 \rangle$ on all sites.

For a general description of the quadrupolar structure, one has to express $\hat{\boldsymbol{z}}_j$ on the $(\hat{\boldsymbol{a}}, \hat{\boldsymbol{b}}, \hat{\boldsymbol{c}})$ trihedron of the cubic crystal: $\hat{\boldsymbol{z}}_j = z_{ja}\hat{\boldsymbol{a}} + z_{jb}\hat{\boldsymbol{b}} + z_{jc}\hat{\boldsymbol{c}}$. This yields the following expressions for the quadrupolar components on the $(\hat{\boldsymbol{a}}, \hat{\boldsymbol{b}}, \hat{\boldsymbol{c}})$ trihedron:

$$\begin{aligned} &\langle O_2^0 \rangle_j = \tfrac{1}{2}[3z_{jc}^2 - 1]Q_0 \\ &\langle O_2^2 \rangle_j = \tfrac{1}{2}[z_{ja}^2 - z_{jb}^2]Q_0 \\ &\langle P_{\alpha\beta} \rangle_j = 0 \qquad\qquad (\alpha\beta = ab, bc, ca). \end{aligned} \tag{3}$$

In the case of a magnetic structure with moments along threefold axes, the local cube's symmetry subgroup to be considered is D_{3d}. The local z-axis is again chosen along the magnetic moment directions $\hat{\boldsymbol{z}}_j$; the x-axis is, for instance, taken in one of the mirror planes containing the z-axis. The quadrupolar representation reduces here into a one-dimensional, $(3z^2-r^2)$, and two two-dimensional, $\{(xy, x^2-y^2), (zx, yz)\}$ irreducible representations. As $(3z^2-r^2)$ is preserved in all the symmetry transformations, the only quadrupolar component which may order, with statistical value Q_0, is again O_2^0. Back to the cube's axes, the corresponding quadrupolar components read as:

$$\begin{aligned} &\langle O_2^0 \rangle_j = 0 \qquad \langle O_2^2 \rangle_j = 0 \\ &\langle P_{\alpha\beta} \rangle_j = \tfrac{1}{2}[z_{j\alpha} z_{j\beta}]Q_0 \qquad (\alpha\beta = ab, bc, ca). \end{aligned} \tag{4}$$

The last case to be considered is the one of a magnetic moment along a twofold axis. Then, the cube's symmetry subgroup to be considered is D_{2h}. Taking the z-axis along the moment direction $\hat{\boldsymbol{z}}_j$, choosing the y-axis along the perpendicular cube's edge, one may

define a local $(\hat{\boldsymbol{x}}_j, \hat{\boldsymbol{y}}_j, \hat{\boldsymbol{z}}_j)$ trihedron at any j site:

$$\begin{aligned}\hat{\boldsymbol{z}}_j &= z_{ja}\hat{\boldsymbol{a}} + z_{jb}\hat{\boldsymbol{b}} + z_{jc}\hat{\boldsymbol{c}}\\ \hat{\boldsymbol{y}}_j &= 2(z_{jb}z_{jc}\hat{\boldsymbol{a}} + z_{jc}z_{ja}\hat{\boldsymbol{b}} + z_{ja}z_{jb}\hat{\boldsymbol{c}})\\ \hat{\boldsymbol{x}}_j &= \hat{\boldsymbol{y}}_j \times \hat{\boldsymbol{z}}_j.\end{aligned}$$

On this trihedron, one observes that the quadrupolar representation reduces into five one-dimensional representations, $\{(3z^2 - r^2), (x^2 - y^2), (xy), (yz), (zx)\}$. Both $(3z^2 - r^2)$ and $(x^2 - y^2)$ correspond to the fully symmetric representation and two quadrupolar components, O_2^0 and O_2^2, are preserved in all the D_{2h} transformations. Thus the ordered quadrupoles may be represented by two scalars $Q_0 = \langle O_2^2 \rangle$ and $Q_1 = \langle O_2^2 \rangle$. Expressing the quadrupolar moments on the cube's trihedron yields:

$$\begin{aligned}\langle O_2^0 \rangle_j &= \tfrac{1}{2}[3z_{jc}^2 - 1]Q_0 + 6[z_{jc}^2(z_{jb}^2 - z_{ja}^2)^2 - z_{ja}^2 z_{jb}^2]Q_1\\ \langle O_2^2 \rangle_j &= \tfrac{1}{2}[z_{ja}^2 - z_{jb}^2]Q_0 + 2[z_{ja}^6 - z_{jb}^6 - 3(z_{ja}^4 - z_{jb}^4) + 2(z_{ja}^2 - z_{jb}^2)]Q_1\\ \langle P_{\alpha\beta} \rangle_j &= \tfrac{1}{2}[z_{j\alpha}z_{j\beta}]Q_0 - 2z_{j\alpha}z_{j\beta}[2(z_{j\alpha}^4 + z_{j\beta}^4) - 4(z_{j\alpha}^2 + z_{j\beta}^2) + 5z_{j\alpha}^2 z_{j\beta}^2 + 2]Q_1\\ &\qquad (\alpha\beta = ab, bc, ca).\end{aligned} \tag{5}$$

As an illustration for the use of these relations between the magnetic and quadrupolar structures, let us consider the simple example of the triple-k magnetic structure stabilized in the NdZn compound [14] (figure 1(a)). The wave vectors are the three independent branches of the $\langle 1/2\,0\,0 \rangle$ star and the moments point along threefold axes. The normalized magnetic structure is easily expressed as:

$$\hat{\boldsymbol{z}}_j = \frac{1}{\sqrt{3}}(\mathrm{e}^{\mathrm{i}\boldsymbol{k}_1\cdot\boldsymbol{R}_j}\hat{\boldsymbol{a}} + \mathrm{e}^{\mathrm{i}\boldsymbol{k}_2\cdot\boldsymbol{R}_j}\hat{\boldsymbol{b}} + \mathrm{e}^{\mathrm{i}\boldsymbol{k}_3\cdot\boldsymbol{R}_j}\hat{\boldsymbol{c}})$$

where $\boldsymbol{k}_1 = [1/2\ 0\ 0]$, $\boldsymbol{k}_2 = [0\ 1/2\ 0]$ and $\boldsymbol{k}_3 = [0\ 0\ 1/2]$ (in $2\pi/a$ units). Using (4) then yields:

$$\begin{aligned}&\langle O_2^0 \rangle_j = 0 \qquad \langle O_2^2 \rangle_j = 0\\ &\langle P_{ab} \rangle_j = Q_0\frac{\mathrm{e}^{\mathrm{i}\boldsymbol{q}_3\cdot\boldsymbol{R}_j}}{6} \qquad \langle P_{bc} \rangle_j = Q_0\frac{\mathrm{e}^{\mathrm{i}\boldsymbol{q}_1\cdot\boldsymbol{R}_j}}{6} \qquad \langle P_{ca} \rangle_j = Q_0\frac{\mathrm{e}^{\mathrm{i}\boldsymbol{q}_2\cdot\boldsymbol{R}_j}}{6}\end{aligned}$$

where the quadrupolar wave vectors are

$$\begin{aligned}\boldsymbol{q}_1 &= \boldsymbol{k}_2 + \boldsymbol{k}_3 = [0\ 1/2\ 1/2]\\ \boldsymbol{q}_2 &= \boldsymbol{k}_3 + \boldsymbol{k}_1 = [1/2\ 0\ 1/2]\\ \boldsymbol{q}_3 &= \boldsymbol{k}_1 + \boldsymbol{k}_2 = [1/2\ 1/2\ 0].\end{aligned}$$

The quadrupolar structure is then of the antiferroquadrupolar type, with a periodicity which differs from the magnetic one, the propagation vectors belonging to the $\langle 1/2\,1/2\,0 \rangle$ star instead of $\langle 1/2\,0\,0 \rangle$. In case of neodymium, the Stevens α_J factor is negative and the electronic distribution has a negative quadrupolar moment along the local quantization axis. Such a distribution may be crudely represented as a uniformly dense sphere squeezed along its z diameter. This has been used for figure 1(b), where this Γ_5 antiferroquadrupolar structure is represented. For this structure, one should expect quadrupolar reflections for scattering vectors obeying the equation $\boldsymbol{Q} = \boldsymbol{H} - \boldsymbol{q}_\mu$, where $\boldsymbol{H}$ belongs to the crystal reciprocal lattice and μ stands for 1, 2 or 3. Whether the corresponding diffraction peaks may actually be measured is answered in the following section.

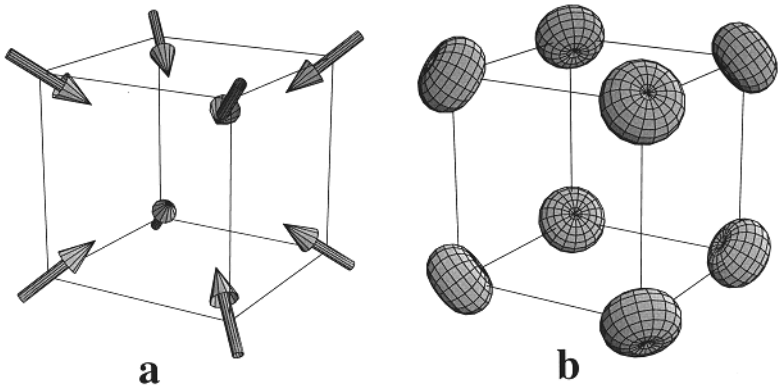

Figure 1. (a) Triple-k magnetic structure of NdZn. (b) The associated antiferroquadrupolar structure.

3. Multipolar x-ray scattering

We consider the simple Thompson scattering of x-rays by the electronic cloud of an atom. Dropping the electronic scattering multiplying factor, the scattering amplitude reduces to the Fourier transform of the electron distribution over the atomic state $|a\rangle$. For a scattering vector $\boldsymbol{Q}$, this scattering amplitude is written

$$A(\boldsymbol{Q}) = \langle a| \sum_j \mathrm{e}^{\mathrm{i}(\boldsymbol{Q}\cdot\boldsymbol{r}_j)}|a\rangle \tag{6}$$

where the index j refers to the electrons of the atom, located at $\boldsymbol{r}_j$.

In the systems which are here of interest, the rare-earth ions are at sites staying as inversion centres, even in the presence of magnetic order. Indeed, a high-symmetry magnetic structure necessarily preserves the inversion symmetry (see equation (1)). Consequently, the expression of the scattering amplitude reduces to

$$A(\boldsymbol{Q}) = \langle a| \sum_j \cos(\boldsymbol{Q}\cdot\boldsymbol{r}_j)|a\rangle.$$

In the same way, the inversion symmetry rules out the existence of any polar vector, in particular, an electric dipole, but also a periodic displacement of the atoms, which would be described by a displacement vector at each site. This is an important remark as then, the observation of x-ray satellites cannot be ascribed to a periodically distorted lattice.

To express the scattering amplitude $A(\boldsymbol{Q})$ in terms of multipolar operators acting on the $|a\rangle$ state, one starts by expanding $\cos(\boldsymbol{Q}\cdot\boldsymbol{r})$ in spherical harmonics. Taking the z axis along the scattering vector $\boldsymbol{Q}$, the expansion reduces to Legendre polynomials of even order. This expansion is summarized in table 2, where the non-zero terms are given up to the sixth order. Higher order terms are useless since their angular integrals over 4f wave functions cancel.

Using this expansion, the scattering amplitude may be reexpressed as a sum of four terms:

$$A(\boldsymbol{Q}) = A_0(\boldsymbol{Q}) + A_2(\boldsymbol{Q}) + A_4(\boldsymbol{Q}) + A_6(\boldsymbol{Q})$$

Table 2. Expansion, to the sixth order ($n = 0, 2, 4, 6$), of $\cos(\boldsymbol{Q}.\boldsymbol{r}\cos\theta)$ in terms of Legendre polynomials. θ is the angle between the scattering vector $\boldsymbol{Q}$ and the position vector $\boldsymbol{r}$ of the jth electron.

n	Polynomial	Radial multiplier $f_n(Qr)$
0	1	$\dfrac{\sin(Qr)}{Qr}$
2	$3\cos^2\theta - 1$	$\dfrac{5}{2}\left[\dfrac{3\cos(Qr)}{Q^2r^2} + \left(1 - \dfrac{3}{Q^2r^2}\right)\dfrac{\sin(Qr)}{Qr}\right]$
4	$35\cos^4\theta - 30\cos^2\theta + 3$	$\dfrac{9}{8}\left[\left(\dfrac{10}{Qr} - \dfrac{105}{Q^3r^3}\right)\dfrac{\cos(Qr)}{Qr} + \left(\dfrac{105}{Q^4r^4} - \dfrac{45}{Q^2r^2} + 1\right)\dfrac{\sin(Qr)}{Qr}\right]$
6	$231\cos^6\theta - 315\cos^4\theta + 105\cos^2\theta - 5$	$\dfrac{13}{16}\left[\left(\dfrac{10\,395}{Q^5r^5} - \dfrac{1260}{Q^3r^3} + \dfrac{21}{Qr}\right)\dfrac{\cos(Qr)}{Qr} + \left(\dfrac{10\,395}{Q^6r^6} + \dfrac{4725}{Q^4r^4} - \dfrac{210}{Q^2r^2} + 1\right)\dfrac{\sin(Qr)}{Qr}\right]$

where

$$A_0(\boldsymbol{Q}) = \langle a| \sum_j f_0(Qr_j)|a\rangle$$
$$A_2(\boldsymbol{Q}) = \langle a| \sum_j f_2(Qr_j)(3\cos^2\theta_j - 1)|a\rangle$$
$$A_4(\boldsymbol{Q}) = \langle a| \sum_j f_4(Qr_j)(35\cos^4\theta_j - 30\cos^2\theta_j + 3)|a\rangle$$
$$A_6(\boldsymbol{Q}) = \langle a| \sum_j f_6(Qr_j)(231\cos^6\theta_j - 315\cos^4\theta_j + 105\cos^2\theta_j - 5)|a\rangle.$$

$A_0(\boldsymbol{Q})$, which includes no angular operator, is the usual scattering amplitude arising from a spherical atom. It is maximum at zero scattering angle, where it is equal to the number of electrons, and is the same on all the identical rare-earth sites. The other terms, which involve angular operators, represent the aspherical contributions to the scattering amplitude. Consequently, in their definition, the sum over the index j can be restricted to the unfilled 4f shell. In contrast with $A_0(\boldsymbol{Q})$, these terms may be periodical, according to the multipolar structure. This should give rise to characteristic interferences resulting in additional Bragg peaks of multipolar origin. The Stevens equivalent-operators method readily applies to these expressions of the second, fourth and sixth order scattering amplitudes, where the radial and angular dependencies are conveniently separated. Comparing the operator defining $A_2(\boldsymbol{Q})$ with the quadrupolar operators of table 1, one finds it may be identified with Q_2^0, apart from the radial dependence where $f_2(Qr_j)$ replaces r_j^2. Thus, the appropriate Stevens equivalent operator is immediately deduced by replacing $\langle r_2\rangle$ by $F_2(Q)$, the 4f radial integral of $f_2(Qr)$:

$$A_2(\boldsymbol{Q}) = \alpha_J F_2(Q)\langle a|O_2^0|a\rangle.$$

$A_2(\boldsymbol{Q})$ is then directly related to the quadrupolar moment along the scattering vector $\boldsymbol{Q}$ and may be referred to as the quadrupolar scattering amplitude. Similarly, introducing the 4f radial integrals, $F_4(Q)$ and $F_6(Q)$, of $f_4(Qr)$ and $f_6(Qr)$, one may rewrite the fourth (octupolar) and sixth order (dodecapolar) scattering amplitudes as

$$A_4(\boldsymbol{Q}) = \beta_J F_4(Q)\langle a|O_4^0|a\rangle$$
$$A_6(\boldsymbol{Q}) = \gamma_J F_6(Q)\langle a|O_6^0|a\rangle$$

where β_J and γ_J are the fourth and sixth order Stevens multiplying factors and $|a\rangle$ the atomic state, expressed using the $|J, J_z\rangle$ base.

Note that the expectation values for the O_2^0, O_4^0 and O_6^0 operators may be rather easily determined within a microscopic magnetic model. In view of a quantitative description of the expected diffraction phenomena, this is a substantial advantage of the $|J, J_z\rangle$ base with regard to the N-electron wave functions.

The $F_2(Q)$, $F_4(Q)$ and $F_6(Q)$ radial integrals act as multipolar scattering form factors. They have been computed using Hartree–Fock (HF) 4f radial wave functions for tripositive rare-earth ions, as defined in [15]. In figures 2, 3 and 4, these multipolar form factors are respectively plotted versus $\sin\theta/\lambda$. In contrast with the spherical scattering amplitude, the multipolar ones are maximum at non-zero scattering angle. This agrees with the calculations of Keating, who started from N-electron determinantal wave functions in the special case of Ho^{3+} [1]. Due to their similar, localized, 4f radial distributions, the different rare-earth ions have their maximum quadrupolar scattering amplitude at about the same scattering angle ($\sin\theta/\lambda \approx 0.5$ Å^{-1}). The maxima of the octupolar and dodecapolar scattering amplitude are further shifted towards higher scattering angles. Non- relativistic HF radial wave functions have here been used for benefit of a simple analytical form. Relativistic effects are not expected to dramatically affect the magnitude of the scattering phenomena but, due to the more expanded 4f radial distribution, to result in a slight shift of the maximum amplitude toward lower scattering angles [16].

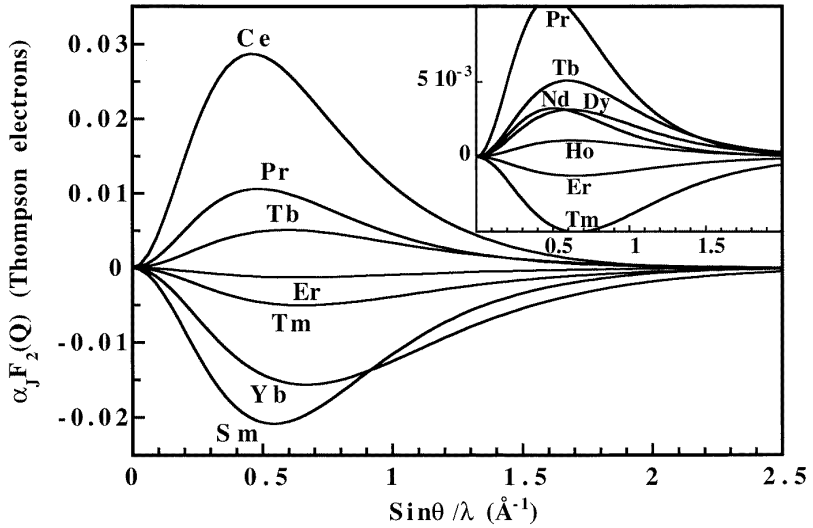

Figure 2. Calculated quadrupolar form factors $\alpha_J F_2(Q)$, as a function of $\sin\theta/\lambda$, for tripositive rare-earth ions. Some curves are displayed in the inset at a more appropriate scale.

For a simple evaluation of the quadrupolar diffraction peak intensities, let us consider a rare-earth ion with its maximum quadrupolar moment along the scattering vector, that is $\langle O_2^0\rangle = J(2J-1)$. For a given Q value, the corresponding maximum quadrupolar scattering amplitude is then $A_2(\boldsymbol{Q}) = \alpha_J F_2(Q) J(2J-1)$. Selecting the scattering vectors maximizing $F_2(Q)$, we have plotted the maximum quadrupolar scattering amplitude which may be expected for the various rare-earth ions (figure 5, in absolute values). In the most favourable case of Tb^{3+}, this scattering amplitude reaches a little less than 0.35 Thompson

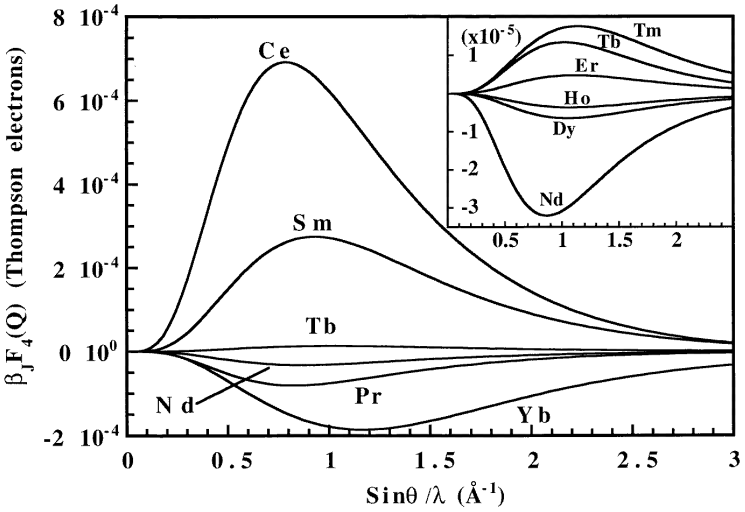

Figure 3. Calculated octupolar form factors $\beta_J F_4(Q)$, as a function of $\sin\theta/\lambda$, for tripositive rare-earth ions. Some curves are displayed in the inset at a more appropriate scale.

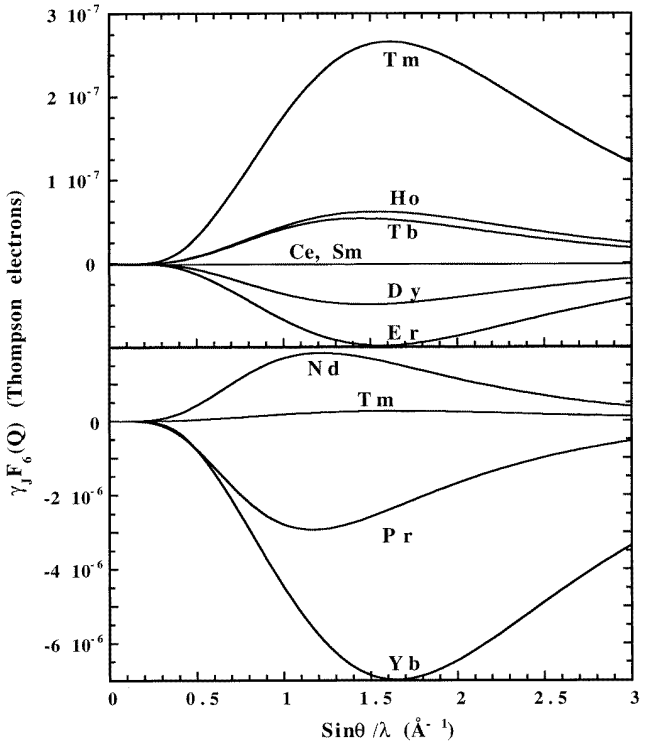

Figure 4. Calculated dodecapolar form factors $\gamma_J F_6(Q)$, as a function of $\sin\theta/\lambda$, for tripositive rare-earth ions.

electron contribution. One may then estimate the maximum ratio between a quadrupolar and a lattice reflection (this latter for zero scattering angle): $R_{\max} = (A_2(Q_{\max})/(Z-3))^2 =$

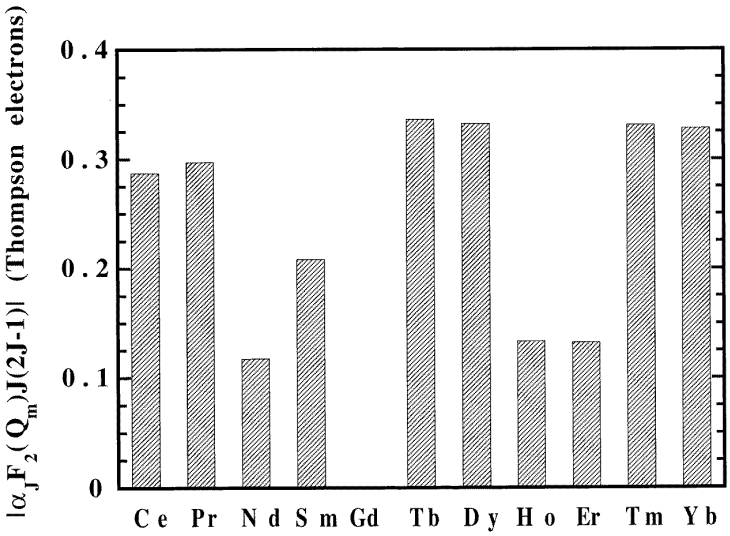

Figure 5. Maximum absolute value of the quadrupolar scattering amplitude for the rare-earth tripositive ions.

$(0.35/62)^2 \approx 3 \times 10^{-5}$. This quadrupolar diffraction phenomenon, which appears three or four orders of magnitude larger than the non-resonant magnetic x-ray diffraction [17], seems to be perfectly measurable. However, it has to be stressed that this ratio is the very maximum which may be expected. In practice, one will have to deal with systems for which, due to thermal disorder or/and crystalline electric field, the quadrupolar moments remain much smaller than their maximum value.

For practical use, the expression for the quadrupolar scattering amplitude needs to be written for any scattering vector referred to the lattice coordinate system. This requires the scattering amplitude to be transformed into the ($\hat{\boldsymbol{a}}$, $\hat{\boldsymbol{b}}$, $\hat{\boldsymbol{c}}$) cube's trihedron, which calls in play the four additional quadrupolar operators:

$$A_2(\boldsymbol{Q}) = \alpha_J F_2(Q) \left[\frac{1}{2} \left(3\frac{Q_c^2}{Q^2} - 1 \right) \langle O_2^0 \rangle + \frac{3}{2} \left(\frac{Q_a^2 - Q_b^2}{Q^2} \right) \langle O_2^2 \rangle + 6 \left(\frac{Q_a Q_b}{Q^2} \langle P_{ab} \rangle + \text{c.p.} \right) \right]. \tag{7}$$

In this expression, the values of the quadrupolar components, over the state $|a\rangle$, have been replaced by the statistical ones. This is the only expression of practical interest, since the total scattered wave will necessarily obey the statistics of the many scattering centres of the crystal.

One may also notice that the expressions of the multiplying factors preceding the quadrupolar operators are very similar to those of the quadrupolar operators themselves. Indeed, this is a common consequence of the symmetries of the Thompson scattering. If one considers an experiment in which both the crystal and the scattering vector are transformed according to a crystal point symmetry operation, the scattering amplitude should be unchanged. Thus, these multiplying factors, which are functions of the scattering vector, should transform exactly in the same way as their corresponding quadrupolar operators.

Equivalent expressions have been written for the octupolar and dodecapolar scattering amplitudes and are reported in the appendix. Thus one may as well compute the fourth

and sixth order contributions to the scattering amplitude. However, in the cubic rare-earth systems, the expectation values for the octupolar and dodecapolar operators mainly result from the crystalline electric field. Consequently, the main contribution to the octupolar and dodecapolar scattering amplitude is constant from site to site and the interference, outside the Brillouin-zone centre, between quadrupolar and higher order multipolar scattering amplitudes may be neglected, this, at least in a first approximation, for scattering angles around the maximum of the quadrupolar scattering amplitude. On a site of cubic symmetry, unlike the octupolar and dodecapolar operators, the quadrupolar operator expectation values result exclusively from pair interactions, dipolar or quadrupolar. Therefore, they may develop with a periodicity potentially different from the lattice one and result in well identifiable diffraction peaks.

4. Summary

The explicit relation between the multiaxial magnetic structure and the associated quadrupolar arrangement has been derived from simple symmetry arguments. Thus the neutron diffraction determination of a magnetic structure also yields, indirectly, the quadrupolar structure. This brings the opportunity of experimenting the x-ray quadrupolar diffraction on well defined quadrupolar arrangements.

In view of this, the Thompson quadrupolar scattering amplitude, as well as the octupolar and dodecapolar ones, have been expressed using the Stevens equivalent-operator method. These scattering amplitudes call into play the respective scattering form factors and a sum of products between multipolar operators and symmetry related combinations of the scattering vector components. This tight relation between the chosen scattering vector and the multipolar operators in the scattering amplitude is a means to determine the actual order parameter, in the case, for instance, of pure antiferroquadrupolar order. Moreover, the use of the ground state multiplet representation gives way to a computational description of the scattering phenomena, starting from an accurate microscopic magnetic model, i.e. accounting for the crystalline electric field and the various pair interactions (see, for example, [18]). In cubic systems, as a first approximation, such an analysis can be restricted to the quadrupolar scattering terms since, out from the zone centre, the fourth and sixth order contributions to the scattering might be neglected. This is reminiscent of the general approximation used in 4f magnetism, for instance, in magnetoelasticity, the analysis of which is usually restricted to second order terms. The contribution to the scattering of conduction electrons of d character may also be neglected. Indeed, the corresponding interference with the 4f quadrupolar scattering should occur at small scattering angles, where the 4f scattering amplitude is already zero. In brief, and without need of further developing such an accurate analysis, our estimate of the quadrupolar diffraction intensity drives us to optimistically consider the outcome of an experimental study.

This needs first the selection of a cubic system suitable for such an experiment. From the quadrupolar diffraction intensities, expected for the tripositive rare-earth ions, one would prefer to deal with a system based on terbium, dysprosium or thulium, for the heavy rare earths, and cerium or praseodymium, for the light ones. This system has to display multiaxial magnetic structures and should also rule out or, at least, reduce the risk of other origins for the expected Bragg peaks. Appropriate multiaxial structures are found among the rare-earth compounds having a simple cubic lattice of magnetic ions and displaying an antiferromagnetism with wave vectors from the $\langle 1/2\ 0\ 0\rangle$ or $\langle 1/2\ 1/2\ 0\rangle$ stars. One might regard as difficult the determination of the actual origin of the measured diffraction signal, for scattering vectors corresponding to the quadrupolar periodicity, as this signal could be

confused with a magnetic one. In the case of a $\langle 1/2\ 0\ 0\rangle$ multiaxial magnetic structure, the occurrence of such a confusion can be immediately rejected, since, as shown by the example of NdZn's triple-k structure, the quadrupolar periodicity differs from the magnetic one. This is however not the case with a $\langle 1/2\ 1/2\ 0\rangle$ multiaxial magnetic structure for which the quadrupolar arrangement has the same periodicity. Nevertheless, as the quadrupolar x-ray scattering intensities are theoretically several orders of magnitude larger than the x-ray magnetic scattering intensities, the confusion of these two scattering phenomena cannot be seriously considered. Actually, the major risk appears to be the confusion with Bragg peaks arising from periodic ion displacements. As already mentioned, this risk is reduced using magnetic high-symmetry structures. Such displacements may nevertheless occur as result of an underlying lattice instability as encountered, for instance, in some rare-earth–silver systems [19]. In case of doubt, the scattering vector dependence and the thermal variation of the observed intensities may allow one to identify their actual origin.

Finally, let us put in more concrete terms the search for a favourable candidate. Within the CsCl-type structure, $\langle 1/2\ 0\ 0\rangle$ magnetic wave vectors are found in the RZn or RMg series [8]. Unfortunately, most of the corresponding magnetic structures are collinear and multiaxial structures are met only for the unfavourable cases of neodymium based compounds, NdZn [14] and NdMg [20].

More numerous are the examples of systems displaying multiaxial magnetic structures based on $\langle 1/2\ 1/2\ 0\rangle$ wave vectors. Among them a number are based on favourable rare earths from the quadrupolar scattering amplitude point of view. For instance, within the CsCl-type structure, one may consider DyCu [21], DyAg [22] or PrAg [23].

Appendix

General expressions of the octupolar, $A_4(\boldsymbol{Q})$, and dodecapolar, $A_6(\boldsymbol{Q})$, scattering amplitudes for a scattering vector $\boldsymbol{Q} = (Q_a, Q_b, Q_c)$ expressed with respect to the cubic lattice trihedron. $\beta_J F_4(Q)$ and $\gamma_J F_6(Q)$ are, respectively, the octupolar and dodecapolar form factors. The definitions of the $O_n^{m(c,s)}$ equivalent operators are given in the text (section 2.2, equations (2)).

$$\begin{aligned}A_4(\boldsymbol{Q}) = \beta_J F_4(Q)[&C_4^0(\boldsymbol{Q})\langle O_4^0\rangle + C_4^{1c}(\boldsymbol{Q})\langle O_4^{1c}\rangle + C_4^{1s}(\boldsymbol{Q})\langle O_4^{1s}\rangle + C_4^{2c}(\boldsymbol{Q})\langle O_4^{2c}\rangle \\ &+C_4^{2s}(\boldsymbol{Q})\langle O_4^{2s}\rangle + C_4^{3c}(\boldsymbol{Q})\langle O_4^{3c}\rangle + C_4^{3s}(\boldsymbol{Q})\langle O_4^{3s}\rangle + C_4^{4c}(\boldsymbol{Q})\langle O_4^{4c}\rangle \\ &+C_4^{4s}(\boldsymbol{Q})\langle O_4^{4s}\rangle]\end{aligned}$$

where

$$\begin{aligned}C_4^0(\boldsymbol{Q}) &= (1/8Q^4)(35Q_c^4 - 30Q^2Q_c^2 + 3Q^4) \\ C_4^{1c}(\boldsymbol{Q}) &= (\sqrt{10}/4Q^4)Q_aQ_b(7Q_c^2 - 3Q^2) \\ C_4^{1s}(\boldsymbol{Q}) &= (\sqrt{10}/4Q^4)Q_bQ_c(7Q_c^2 - 3Q^2) \\ C_4^{2c}(\boldsymbol{Q}) &= (\sqrt{5}/4Q^4)(Q_a^2 - Q_b^2)(7Q_c^2 - Q^2) \\ C_4^{2s}(\boldsymbol{Q}) &= (\sqrt{5}/4Q^4)2Q_aQ_b(7Q_c^2 - Q^2) \\ C_4^{3c}(\boldsymbol{Q}) &= (\sqrt{35}/\sqrt{8}Q^4)Q_c(Q_a^3 - 3Q_aQ_b^2) \\ C_4^{3s}(\boldsymbol{Q}) &= (\sqrt{35}/\sqrt{8}Q^4)Q_c(3Q_bQ_a^2 - Q_b^3) \\ C_4^{4c}(\boldsymbol{Q}) &= (\sqrt{35}/8Q^4)(Q_a^4 - 6Q_a^2Q_b^2 + Q_b^4) \\ C_4^{4s}(\boldsymbol{Q}) &= (\sqrt{35}/8Q^4)4Q_aQ_b(Q_a^2 - Q_b^2)\end{aligned}$$

$$A_6(\boldsymbol{Q}) = \gamma_J F_6(Q)[C_6^0(\boldsymbol{Q})\langle O_6^0\rangle + C_6^{1c}(\boldsymbol{Q})\langle O_6^{1c}\rangle + C_6^{1s}(\boldsymbol{Q})\langle O_6^{1s}\rangle + C_6^{2c}(\boldsymbol{Q})\langle O_6^{2c}\rangle + C_6^{2s}(\boldsymbol{Q})\langle O_6^{2s}\rangle + C_6^{3c}(\boldsymbol{Q})\langle O_6^{3c}\rangle + C_6^{3s}(\boldsymbol{Q})\langle O_6^{3s}\rangle + C_6^{4c}(\boldsymbol{Q})\langle O_6^{4c}\rangle + C_6^{4s}(\boldsymbol{Q})\langle O_6^{4s}\rangle + C_6^{5c}(\boldsymbol{Q})\langle O_6^{5c}\rangle + C_6^{5s}(\boldsymbol{Q})\langle O_6^{5s}\rangle + C_6^{6c}(\boldsymbol{Q})\langle O_6^{6c}\rangle + C_6^{6s}(\boldsymbol{Q})\langle O_6^{6s}\rangle]$$

where

$$C_6^0(\boldsymbol{Q}) = (1/16Q^6)(231Q_c^6 - 315Q_c^4Q^2 + 105Q_c^2Q^4 - 5Q^6)$$
$$C_6^{1c}(\boldsymbol{Q}) = (\sqrt{21}/8Q^6)Q_a(33Q_c^5 - 30Q_c^3Q^2 + 5Q_cQ^4)$$
$$C_6^{1s}(\boldsymbol{Q}) = (\sqrt{21}/8Q^6)Q_b(33Q_c^5 - 30Q_c^3Q^2 + 5Q_cQ^4)$$
$$C_6^{2c}(\boldsymbol{Q}) = -(\sqrt{210}/256Q^6)(Q_a^2 - Q_b^2)(33Q_c^4 - 18Q_c^2Q^2 + Q^4)$$
$$C_6^{2s}(\boldsymbol{Q}) = -(\sqrt{210}/256Q^6)2Q_aQ_b(33Q_c^4 - 18Q_c^2Q^2 + Q^4)$$
$$C_6^{3c}(\boldsymbol{Q}) = (\sqrt{105}/\sqrt{128}Q^6)Q_aQ_c(3Q_b^2 - Q_a^2)(11Q_c^2 - 3Q^2)$$
$$C_6^{3s}(\boldsymbol{Q}) = (\sqrt{105}/\sqrt{128}Q^6)Q_bQ_c(3Q_a^2 - Q_b^2)(3Q^2 - 11Q_c^2)$$
$$C_6^{4c}(\boldsymbol{Q}) = (\sqrt{7}/48Q^6)(Q_a^4 - 6Q_a^2Q_b^2 + Q_b^4)(11Q_c^2 - Q^2)$$
$$C_6^{4s}(\boldsymbol{Q}) = (\sqrt{7}/48Q^6)Q_aQ_b(Q_a^2 - Q_b^2)(11Q_c^2 - Q^2)$$
$$C_6^{5c}(\boldsymbol{Q}) = (3\sqrt{154}/16Q^6)Q_aQ_c(Q_a^4 - 10Q_a^2Q_b^2 + 5Q_b^4)$$
$$C_6^{5s}(\boldsymbol{Q}) = (3\sqrt{154}/16Q^6)Q_bQ_c(Q_b^4 - 10Q_a^2Q_b^2 + 5Q_a^4)$$
$$C_6^{6c}(\boldsymbol{Q}) = (\sqrt{231}/16\sqrt{2}Q^6)(Q_a^6 - 15Q_a^4Q_b^2 + 15Q_a^2Q_b^4 - Q_b^6)$$
$$C_6^{6s}(\boldsymbol{Q}) = (\sqrt{231}/16\sqrt{2}Q^6)Q_aQ_b(3Q_a^4 - 10Q_a^2Q_b^2 + 3Q_b^4).$$

References

[1] Keating D T 1969 *Phys. Rev.* **178** 732
[2] Levy P M, Morin P and Schmitt D 1979 *Phys. Rev. Lett.* **42** 1417
[3] Aléonard R and Morin P 1979 *Phys. Rev.* B **19** 3868
[4] Felcher G P, Lander G H, Arai T, Sinha S K and Spedding F H 1976 *Phys. Rev.* B **13** 3034
[5] Effantin J M, Rossat-Mignod J, Burlet P, Bartholin H, Kunii S and Kasuya T 1985 *J. Magn. Magn. Mater.* **47/48** 145
[6] Uimin G 1997 *Phys. Rev.* B **55** 8267
[7] Walker M B, Kappler C, McEwen K A, Steigenberger U and Clausen K N 1994 *J. Phys.: Condens. Matter* **6** 7365
[8] Morin P and Schmitt D 1990 *Ferromagnetic Materials* vol 5, ed K H J Buschow and E P Wohlfarth (North-Holland: Amsterdam) p 1
[9] Matsumura T, Haga Y, Nemoto Y, Nakamura S, Goto T and Suzuki T 1995 *Physica* B **206/207** 380
[10] Amara M and Morin P 1995 *Physica* B **205** 379
[11] Stevens K H W 1952 *Proc. Phys. Soc.* A **65** 209
[12] Hutchings M T 1964 *Solid State Physics* vol 23 (New York: Academic) p 283
[13] Buckmaster H A 1962 *Can. J. Phys.* **49** 1670
[14] Amara M, Morin P and Burlet P 1995 *Physica* B **210** 157
[15] Freeman A J and Watson R E 1962 *Phys. Rev.* **127** 2058
[16] Freeman A J and Desclaux J P 1979 *J. Magn. Magn. Mater.* **12** 11
[17] Blume M 1985 *J. Appl. Phys.* **57** 3615
[18] Amara M and Morin P 1996 *Physica* B **222** 61
[19] Abu-Aljarayesh I, Kouvel J S and Brun T O 1986 *Phys. Rev.* B **34** 240
[20] Deldem M, Amara M, Galéra R M, Morin P, Schmitt D and Ouladdiaf B 1998 *J. Phys.: Condens. Matter* **10** 165
[21] Amara M, Morin P and Bourdarot F 1997 *J. Phys.: Condens. Matter* **9** 7441
[22] Morin P, Rouchy J, Yonenobu K, Yamagishi A and Date M 1989 *J. Magn. Magn. Mater.* **81** 247
[23] Morin P and Schmitt D 1982 *Phys. Rev.* B **26** 3891